Electron-impurity scattering rates of dilute alloys of Cu as measured by surface-state resonances

A. J. Baratta
Pennsylvania State University, Univeristy Park, Pennsylvania 16802

A. C. Ehrlich
Naval Research Laboratory, Washington, D.C. 20375

(Received 2 May 1983)

A method for studying the electron-impurity scattering rate by magnetic-field-induced surface-state resonances (SSR) in Cu alloys in the presence of overlapping signals is outlined and compared to temperature dependent de Haas—van Alphen techniques. Experiments using the SSR technique in the (110) sample plane in *Cu*Ni alloys are reported. The scattering rate induced by the Ni impurity is found to vary by a factor of 5 over the Fermi surface. The variation follows closely the magnitude of the *d*-wave component of the electron wave functions in Cu as determined from band-structure calculations. It is concluded that the scattering potential introduced by Ni in Cu connects primarily the *d* states. The relevance of the scattering anisotropy to the existing Hall-effect data is also discussed.

I. INTRODUCTION

The significance of the anisotropic scattering of conduction electrons in a metal is well recognized.[1] The anisotropy provides an explanation for a variety of properties. These include, for example, the variation of the Hall effect upon alloying. Similarly, other transport properties such as magnetoresistance are also sensitive to the anisotropy.

A number of experimental methods exist that provide for the measurement of the anisotropy of the scattering. Of these, the surface-state scattering technique is the most direct.[2–5] In this paper we report on the experimental measurement of the anisotropic scattering due to a Ni impurity in Cu using the surface-state resonance technique. These results are compared with those obtained earlier by the authors for an Al impurity in Cu (Ref. 6) and with those obtained for Ni by others from de Haas—van Alphen (dHvA) effect studies.[7,8]

Magnetic-field-induced surface-state resonances provide a unique and powerful technique to study the anisotropy of electron scattering interactions in metals and semimetals. Like the dHvA effect, surface-state resonances yield detailed and local information pertaining to scattering rates.[9] In the sections that follow we describe how magnetic-field-induced surface-state resonances can be used to determine electron scattering rates and how the experimental data is handled to achieve this. This is particularly relevant in as much as there has been no previous description of analysis of data consisting of overlapping lines. We also compare the surface-state method to dHvA techniques. In the final section the electron scattering rates are presented and compared with dHvA results. Implications are drawn regarding the anisotropy and its relationship to the variation of the electron wave function over the Fermi surface and to the variation in the Hall effect upon alloying.

II. THEORETICAL BACKGROUND

Classically, magnetic-field-induced surface-state resonances correspond to electrons moving along the surface with a periodic skipping motion (Fig. 1). The electrons are constrained to the near-surface region by the Lorentz force associated with the applied magnetic fields. The orbits are quantized with the maximum penetration depth given by[4]

$$Z_n=(a_n)^{2/3}(h/e)^{1/3}\frac{1}{H^{1/3}K_\perp^{1/3}},$$

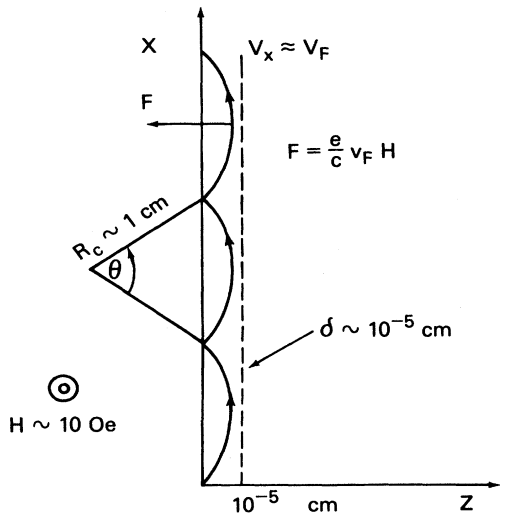

FIG. 1. Schematic representation of surface states showing electron skipping trajectory induced by the applied magnetic field H. R_c is the radius of curvature of the electron orbit, V_f is the Fermi velocity, and δ is the skin depth. θ is typically 1°—2°.

where a_n is the nth zero of the Airy function [$\mathrm{Ai}(-a_n)=0$, $n=1,2$,etc., Ai is the airy function], H is the magnitude of the applied magnetic field, and K is the local radius of curvature of the Fermi surface. The symbol $\perp$ denotes the projection of the Fermi-surface radius of curvature in the plane perpendicular to the applied magnetic field. The energy levels for the surface are given by

$$E_n=(a_n)^{2/3}(e^2h)^{1/3}H^{2/3}(V_f/K^{1/3})_\perp ,$$

where V_f is the Fermi velocity and the symbol $\perp$ denotes the component of the Fermi velocity and the radius of curvature in the plane perpendicular to the applied magnetic field.

If the sample is placed in a microwave field polarized such that the electric field vector has a nonzero component parallel to the Fermi velocity, then transitions between surface states can be induced. For a fixed microwave frequency ω, resonant transitions are expected whenever the magnetic field H is such that the energy separation of the surface-state levels m and n satisfies the Einstein relation

$$\hbar\omega=E_m-E_n .$$

The resonant magnetic field H_{mn} is then given by

$$H_{mn}=\frac{\hbar}{e}\left[\frac{\omega}{a_n-a_m}\right]^{3/2}\left[\frac{2K}{V_f^3}\right]_\perp^{1/2} .$$

The resonances are observed as changes in the microwave surface impedance of the metal. If one plots the derivative of the real part of surface impedance with respect to the applied magnetic field, dR/dH, one finds peaks that occur near the resonant magnetic fields H_{mn}. Figure 2 illustrates a typical surface-state signal. Shown is a spectrum from the (110) plane of Cu.

The electron states that contribute to a given resonance signal are those for which the resonance parameter

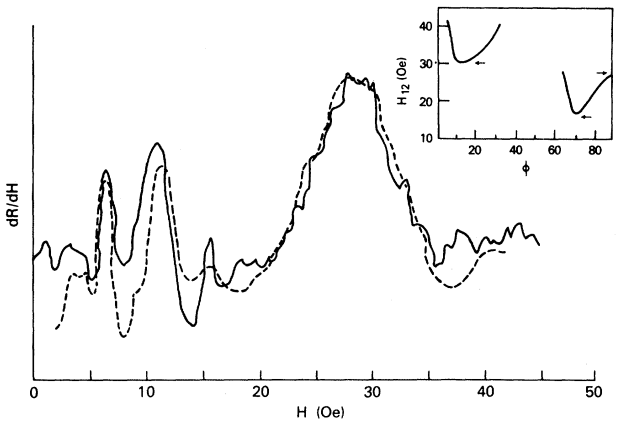

FIG. 2. Comparison of the experimental resonance spectrum (solid line) in Cu with that predicted by theory (dashed line) for H parallel to $\langle 100\rangle$ and the rf electric field parallel to H. Inset depicts predicted minima and maximum in plot of resonant field value for transition between first and second surface-state energy levels. Angle ϕ is measured from $\langle 100\rangle$ axis with respect to the center of the Brillouin zone in the (110) plane.

$(K/V_f^3)_\perp^{1/2}$ has a local extremum and whose Fermi velocity is approximately parallel to the sample surface.[10] Typically, these regions are 3°—10° in length and 0.5°—2° in width with respect to the center of the Brillouin zone. Hence the various parameters, including the scattering rates, obtained from an analysis of surface-state resonances are associated with very small regions of the Fermi surface.

By comparison, the scattering rate obtained from dHvA measurements are not local to a particular region on the Fermi surface. Instead, they are averages relating to electron states lying along narrow, well-defined extremal orbits on the Fermi surface. As assumed by Lowndes[11] the orbital values for the scattering rate are related to the point-by-point scattering rates by the relation

$$\langle 1/\tau_s\rangle=T_0^{-1}\oint\frac{dt}{\tau_s(t)} ,$$

where T_0 is the cyclotron time, $\tau_s(t)$ is the point-by-point scattering time, and the integral is performed over the dHvA orbit. The orbital averages are thus the local values weighted by the amount of time dt spent at a particular point on the Fermi surface. To obtain point-by-point estimates of the scattering rates, it is necessary to invert the integral above.

The inversion may be accomplished provided a comprehensive set of orbital scattering rates are available from dHvA measurements.[12] The process involves assuming a representation $\tau_s(\vec{k},C_i)$ for the scattering rates. The cubic harmonic and symmetrized Fourier series expansions have been used for this purpose.[12] The parameter C_i depends upon the specific representation. Regardless of the representation used, the coefficients are determined by an iterative least-squares fitting of the calculated orbital averages to those experimentally determined. The number of coefficients that can be obtained is limited to the number of different orbits for which data is available.

The inversion process results in the introduction of uncertainties in the point-by-point estimates of the scattering rate. Poulsen *et al.*[7] have estimated the uncertainties in the inversion by determining the variation in the local scattering rate as a function of the number of coefficients. The number of Fourier coefficients was increased from 3 to 7. For various Cu alloys the resulting uncertainties ranged from a few percent for the neck region to 50—100 % for points around the $\langle 100\rangle$ axis.

The experimental measurement of scattering rate involves the measurement of the amplitude variation of the harmonics of the dHvA signal. The nth harmonic is reduced by a factor $\exp(-nKm_cx/H)$, where n is the index of the harmonic, K is a constant, 146.9 $\mathrm{Kg\,K^{-1}}$, m_c is the cyclotron effective mass in units of free-electron mass, H is the magnetic field, and x is the Dingle temperature. The Dingle temperature is related to the average (around the dHvA orbit) of the scattering rate by

$$x=\frac{h}{2\pi k_B}\langle 1/\tau\rangle .$$

The above assumes that only one extremal orbit contributes to the signal. If more than one is present, one ob-

tains overlapping signals with a much more complex variation in the amplitude behavior of the harmonics. Techniques are available for extracting the Dingle temperatures and hence the scattering rate for such cases.[13]

The extraction of point-by-point estimates of the electron scattering rates from magnetic induced surface-state resonances do not involve such inversion schemes. Rather, the width of the dR/dH peaks are directly related to the point-by-point scattering rates. Doezema and Koch[9] have shown empirically that for the $n=1$ to $m=2$ transition, the scattering rate is related to the relative width at half-amplitude $\Delta H/H$ by

$$[1/\tau(k)]_{\mathrm{av}}=\frac{\omega}{1.56}\left[\frac{\Delta H}{H}-0.02\right],$$

where ω is the microwave frequency and the square brackets denote an average over the aforementioned strip. The strip length over which the scattering rate is averaged may be estimated by the variation in the resonance parameter $(K/V_f^3)_\perp^{1/2}$ around the extremal point. For Cu the strip length varies from $10^{-2}k_F$ to $10^{-1}k_F$ where k_F is the magnitude of the Fermi-wave vector.[14]

As in the case of dHvA signals, the above assumes that only one extremum contributes to the surface-state signal. If more than one signal is present, the simple relationship between the apparent linewidth and scattering rate is no longer valid. To our knowledge we are the first to develop and apply a procedure to obtain scattering rates from such signals which is as follows. One first carefully constructs theoretical line shapes which contain contributions from each surface-state signal. The resulting theoretical spectrum is then compared to the experimental date. This process is repeated until a satisfactory fit is obtained.

To understand this process consider the following. The shape of the resonance spectrum is given to a good approximation by[2,3]

$$\mathrm{Re}\left[\frac{dZ}{dH}\right]=\mathrm{Re}\left[\mathrm{const}(i-\sqrt{3})\frac{d}{dH}\int dk_y\left[\frac{V_v^2(k_y)}{V_f(k_y)}\sum_{m,n}\frac{\alpha_{mn}^2(k_y,H,\delta)}{\omega-\omega_{mn}(H,k_y)+i\Gamma(k_y,H)}\right]\right],$$

where k_y is the $\vec{k}$-space coordinate along the magnetic field. The quantity α_{mn} is the matrix element of the electric field between surface-state wave functions in the anomalous—skin-effect skin depth δ of the metal. The quantity V_v is the component of the Fermi velocity V_f along the applied rf electric field and ω_{mn} is the difference in energy between surface states divided by $\hbar$. The dispersive term $i\Gamma$ accounts for electron scattering. The integration over k_y is carried out over the region of the Fermi surface for which an extremum in the resonance parameter $(K/V_f^3)_\perp^{1/2}$ exists using the techniques developed by Koch and Jensen.[15] The scattering rate Γ is adjusted until satisfactory agreement is obtained between the theoretical line shape described by the above expression and the measured data.

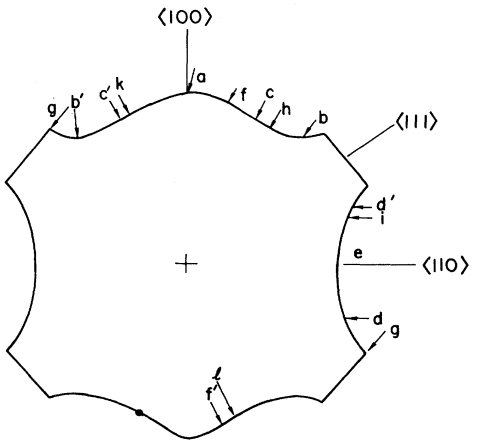

FIG. 3. Fermi-surface regions in the (110) plane of Cu that give rise to surface-state resonances (Ref. 10). Arrows denote the approximate region of the Fermi surface contributing to the signal.

If more than one region of the Fermi surface exhibits an extremum then the contribution from each must be accounted for. To do this, one carefully chooses appropriate rf electric field and magnetic field orientations such that a minimum number of overlapping signals contribute. For example, in Cu and its alloys, by orienting the magnetic and the electric fields parallel to the ⟨100⟩ axis only the region around f (see Fig. 3) contributes to observed signals. Only this region contributes since the V_v is essentially zero for all other extermal regions. If the electric field is reoriented to lie along the ⟨110⟩ axis, then regions around f, d', and e contribute. Since the scattering rate for region f may be obtained by itself, one then can use it to obtain those for d' and e. Fortuitously, the primary 1-2 transitions for these two regions are separated sufficiently in field so that there is minimal overlap. As a result one can fit these regions separately. The resulting resonance lines are then added together to obtain a theoretical spectrum which is compared to the experimentally obtained one. As in the case of a single resonance, the scattering rates are adjusted until a satisfactory fit of the total theoretical spectrum with the experimental one is obtained. From this process one thus obtains averages for the scattering rates for each of the very localized strips of the Fermi surface which contribute to the observed signals.

III. EXPERIMENT

A. Apparatus

The magnetic-field-induced surface-state measurements were made in a simple set of Helmholtz coils with a maximum field of 120 Oe. A sample holder was used which allowed the rotation of the magnetic field through 360° about an axis perpendicular to the sample plane. The

sample formed one wall of a cylindrical microwave cavity. The change in sample surface impedance was detected by measurement of cavity Q using a conventional reflection-type microwave spectrometer operating at 24 GHz.[9] The magnetic field was modulated at a frequency of 100 Hz to allow synchronous detection of the resulting signal and direct measurment of dR/dH. The work was conducted at liquid-He temperature (nominally 4.2 K).

B. Samples

The Cu sample used in the experiment was spark-cut from a large single-crystal boule. The starting crystal, nominally 99.999% pure, was obtained from Materials Research Corporation. After spark-cutting the Cu sample was annealed in oxygen atmosphere (pressure 4×10^{-4} mm Hg) for 10 d at 1000 °C. The oxygen anneal sequesters the residual impurities rendering them ineffective as electron scattering centers.

After annealing, the sample was boiled for 20 min in a saturated solution of NH_4OH to remove the tightly adherent oxide coating formed during the oxygen anneal. The sample was then mechanically lapped first using 600-grit paper followed by aluminum oxide. After lapping and immediately prior to measurement the sample was electropolished in a 2:1 solution of H_3PO_4 and water according to the recipe given by Tegart.[16] As reported elsewhere,[6,10] electropolishing times of 4—5 h were required to obtain satisfactory results. Baseline-scattering-rate data were then obtained from the pure-Cu sample.

The Cu(Ni) sample was obtained by diffusion of the Ni impurity into the pure-Cu sample described previously. A thin layer of nickel was vacuum-evaporated onto the polished, oxygen-annealed pure-Cu surface. The nickel was then diffused into the Cu using a high-temperature anneal. The anneal was performed by annealing the Ni-coated Cu sample in vacuum at 790 °C for 373.5 h. After annealing the sample was electropolished to a predetermined depth to obtain the desired Ni concentration. Using diffusion theory it is estimated that the resulting Ni concentration was between 1 and 10 ppm.[17]

C. Scattering-rate measurements and analysis in Cu and Cu(Ni)

Scattering-rate measurements were made for a variety of points on the Fermi surface of the pure Cu and Cu(Ni) samples. Extraction of the scattering rates was done by fitting the theoretical spectrum to the experimentally obtained data. The actual technique used is described elsewhere[6] and will be only briefly reviewed here.

Essentially, the scattering rate is treated as an adjustable parameter. Theoretical spectra are chosen which approximate the experimentally obtained spectra. Final choice of the spectrum which gives the best fit to the experimental data is made by graphic comparison of the actual observed resonance spectrum to the theoretical ones. The scattering-rate value of the theoretical spectrum which gave rise to the best fit is then chosen as the value for that region of the Fermi surface from which the lines originated. The various regions of the Fermi surface from which signals can be observed are shown in Fig. 3.

D. Experimental results

Scattering rates before and after alloying with Ni were obtained. A series of 10 spectra from the (110) sample plane of Cu and Cu(Ni) were obtained and analyzed. Figure 4 shows a typical spectrum prior to and after alloying. The dramatic change is evident. Shown are resonant spectra from the (110) sample plane of pure Cu and Cu(Ni). The magnetic field is along the ⟨110⟩ axis. The microwave electric field is along the ⟨100⟩ axis. Signals that contribute to the observed spectrum originate from the Fermi surface near the ⟨100⟩ axis and from regions midway between the ⟨100⟩ axis and the ⟨111⟩ axis.

Table I summarizes the resulting changes in scattering rate upon alloying. The scattering rate Γ^* ($\Gamma^*=1/\omega\tau$) is given for the (110) planes of Cu and Cu(Ni) as a function of the angle θ that the applied magnetic field makes with the ⟨110⟩ axis in the sample plane. The angle ϕ taken with respect to the ⟨100⟩ direction locates the region of the Fermi surface which gives rise to the signal. The angle $\Delta\phi$ measures the strip width over which there is a significant contribution to the observed resonance spectrum. The quantity $\Delta\Gamma^*$ is the change in scattering rate upon alloying with Ni. The angle ψ indicates the angle the rf electric field makes with the ⟨100⟩ axis.

Figure 5 shows the change in scattering rate $\Delta\Gamma^*$ as a function of Fermi-surface location. Again the angle ϕ is taken with respect to the ⟨100⟩ axis and the center of the Brillouin zone. Unfortunately, no data could be obtained for points between the ⟨111⟩ and the ⟨110⟩ axis due to the large amount of electron scattering which occurred in the alloyed sample.

The anisotropy observed with magnetic-field-induced surface-state resonances is consistent with that obtained from dHvA measurements by Coleridge.[8] These measurements were obtained from the variation in the Dingle temperature x over the Cu Fermi surface and are shown in Fig. 5. Allowing for the uncertainties in the quoted dHvA measurements and the uncertainties in the surface-state measurements, the two sets are seen to be in excellent agreement. Such comparison demonstrates the reliability of both techniques.

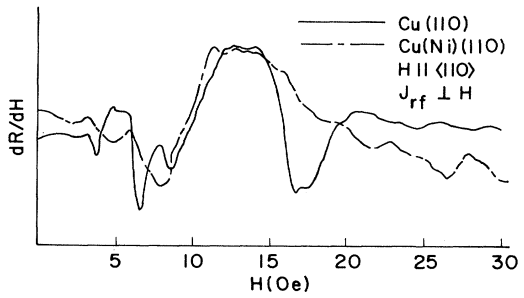

FIG. 4. Comparison of magnetic-field-induced surface-state resonances in Cu (solid line) and Cu(Ni) (dashed line). H is parallel to the ⟨110⟩ axis and the microwave electric field is parallel to the ⟨100⟩ axis.

TABLE I. Γ^* results for the (110) plane in Cu and Cu(Ni) vs θ, the angle the magnetic field makes with the ⟨110⟩ axis. Angle ϕ is measured from the ⟨100⟩ direction and locates the contributing electrons. Angle $\Delta\phi$ is a measure of the strip width over which there are significant contributions to Γ^*. Angle ψ locates the orientation of the rf electric field relative to the ⟨100⟩ direction.

θ (deg)	ϕ (deg)	$\Delta\phi$ (deg)	ψ (deg)	Γ^* (Cu)	Γ^* [Cu(Ni)]	$\Delta\Gamma^*$
0	0	0 − 7.5	−25	0.17	0.2	0.03
	22.5	10 −27.5		0.16	0.33	0.17
	0	0 − 7.5	0	0.14	0.2	0.06
	22.5	10 −27.5		0.2	0.33	0.13
	40	27.5−42.5		0.17	0.25	0.08
10	3	0 −10	−25	0.17	0.2	0.03
	22.5	10 −30		0.2	0.33	0.13
	23	10 −30		0.2	0.33	0.13
	40	30 −41.5		0.14	0.2	0.06
	40	30 −41.5		0.14	0.2	0.06
	3	0 −10	0	0.14		
	22.5	10 −30		0.2		
	23	10 −30		0.2		
	40	30 −41.5		0.17		
	40	30 −41.5		0.17		
20	5.5	0 −14	−25	0.2	0.25	0.05
	21.5	10.5−38		0.2	0.33	0.13
	24.5	14 −30		0.2	0.33	0.13
	35	30 −41.5		0.2	0.33	0.13
	40	38 −42.5		0.14	0.2	0.06

IV. DISCUSSION

A. Scattering anisotropy

The change in scattering rate upon alloying is found to vary markedly as one moves about the Fermi surface. For CuNi it is lowest for electron states nearest the ⟨100⟩ and ⟨111⟩ neck regions and highest for regions around $\phi=20°-30°$. The measured change in scattering rate is found to vary by a factor of 5 in this region. There is also a smooth variation of the change in scattering rate as one moves from the ⟨100⟩ to ⟨111⟩ axis.

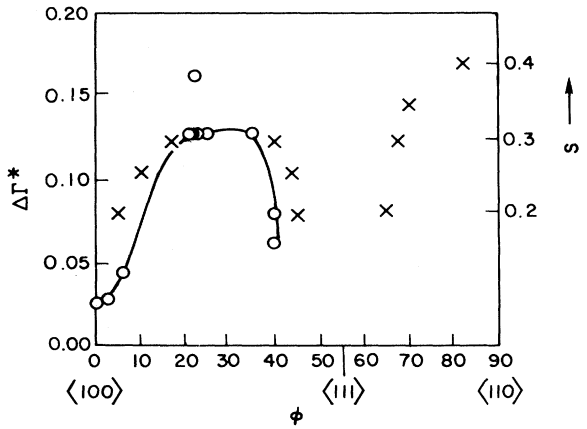

FIG. 5. Comparison of $\Delta\Gamma^*$ in Cu(Ni) as a function of Fermi-surface location to deduced variation of total scattering rate S from dHvA studies of Cu(Ni). ○ denotes this study and × denotes that of Coleridge (Ref. 8).

The anisotropy observed in Cu(Ni) is quite different from that seen in Cu(Al). Figure 6 shows the anisotropy in Cu(Al) as measured by the authors using magnetic induced surface states[6] and by Coleridge and Templeton using the dHvA effect.[8,18] As may be seen, the scattering in Cu(Ni) is a maximum where the scattering in Cu(Al) is a minimum ($\phi=20°-30°$). Also, the electron states near the ⟨100⟩ and ⟨111⟩ axes are scattered least in Cu(Ni) whereas in Cu(Al) they are scattered the most.

B. Effect of anisotropy on the Hall coefficient

The anisotropy of electron scattering plays a critical role in all-electron transport phenomena. A particularly interesting observation may be made regarding the significance of the scattering-rate anisotropy by examining the anisotropy's effect on the Hall coefficient. To do this in a simple way, consider the expression due to Tsuji[19] for the low-field Hall coefficient in a cubic metal with anisotropic scattering time

$$R=\frac{12\pi^3}{ce}\int\frac{\tau^2(\vec{k})V^2[(1/\rho)]_{av}dS}{[\tau(\vec{k})VdS]^2}\,.$$

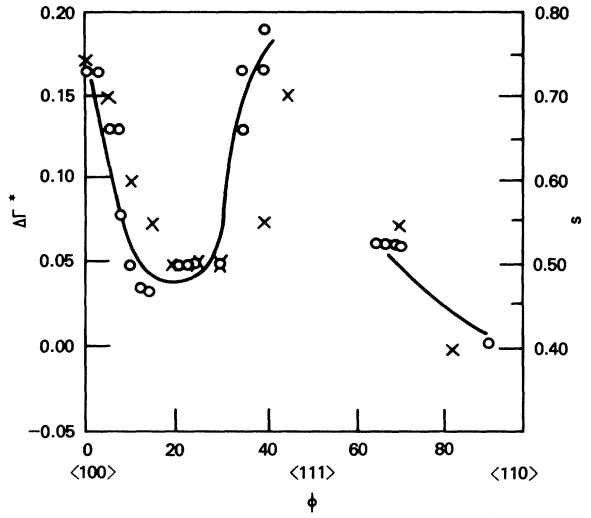

FIG. 6. $\Delta\Gamma^*$ in Cu(Al) as a function of Fermi-surface location from magnetic-field-induced surface-state resonances (Ref. 6). ○ denotes this study and × denotes that of Coleridge (Ref. 8).

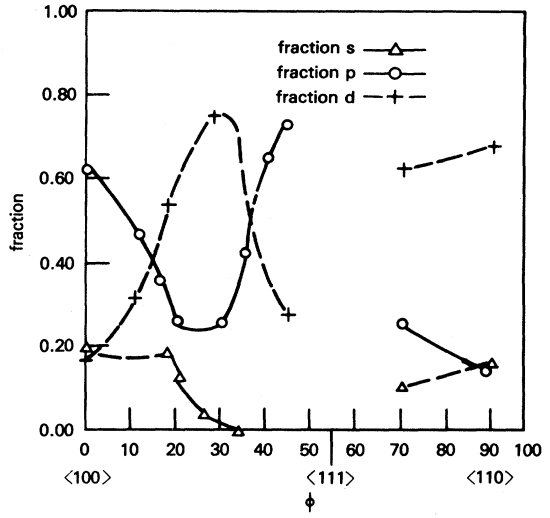

FIG. 7. Fraction of s, p, and d states in the Cu electron wave function vs Fermi-surface location ϕ in the (110) plane measured with respect to the ⟨100⟩ axis from the center of the zone.

Here $\tau(\vec{k})$ is the scattering time at a point on the Fermi surface, V is the Fermi velocity, and $[1/\rho]_{av}=\frac{1}{2}(1/\rho_1+1/\rho_2)$ where ρ_1 and ρ_2 are the principal radii of curvature of the Fermi surface at the point considered. Further we define the reduced Hall coefficient as

$$r=R/R_{FE}\ ,$$

where R_{FE} is the free-electron (FE) Hall coefficient.

If the Tsuji expression for the Hall coefficient is evaluated within the two-band model, one obtains for the reduced Hall coefficient

$$r=4\pi\frac{\tau_B^2\int_B[(1/\rho)]_{av}V^2dS+\tau_N^2\int_N[(1/\rho)]_{av}V^2dS}{\left[\tau_B\int_B V\,dS+\tau_N\int_N V\,dS\right]^2}\ ,$$

where ρ and S are here expressed in terms of the Fermi-surface radius for a free-electron metal with one electron per atom. The quantities τ_B and τ_N are averaged scattering times ascribed to the belly and neck areas, respectively. Typically, the neck area is defined as lying within an angle of 20° from the ⟨111⟩ direction.

Dugdale and Firth[20] used the two-band expression to evaluate the dependence of the reduced Hall coefficient on the ratio of τ_B to τ_N. With the use of measured values of the low-temperature Hall coefficient in Cu(Ni) alloys of various concentrations, Dugdale and Firth also obtained an extrapolated value of the characteristic Hall coefficient of -6.0×10^{-11} m^{3}c^{-1}. This gives a reduced Hall coefficient of 0.8. In combination with the two-band model this suggests that the anisotropy of τ_N to τ_B is then 0.7 or $\tau_N<\tau_B$. They note that this is inconsistent with the Dingle-temperature data from dHvA measurements which predicts a ratio of about 2.0.

To resolve this discrepancy, they suggest that the marked bulging of the Fermi surface near the ⟨100⟩ direction tends to make a larger contribution than can be accounted for in a two-band model. Therefore, they conclude that a three-band model may be needed in which average scattering ratios around the neck regions τ_N, ⟨100⟩ directions τ_{100}, and around the belly regions τ_B, must all be considered. With the use of this model and the Hall-effect data they obtain scattering anisotropies consistent with Dingle-temperature measurements.

The use of the two-band model by Dugdale and Firth is consistent with a history of differentiating the properties of the neck electrons from the rest of the electrons in the noble metals. Dugdale and Basinski,[21] for example, were able in this way to interpret the deviations from Matthiesen's rule in a large number of noble-metal alloys. In fact our results on the variation of the electron scattering rate over the Fermi surface show the variation to be continuous and large, reaching factors of 4 or 5. The size of the anisotropy indicates that the scattering anisotropy is even more important than the Fermi-surface shape anisotropy. This is particularly true for the Hall effect since τ enters as the square while ρ enters as the first power. The more or less continuous variation of the scattering rate emphasizes the artificiality of a two- or even three-band model. Nevertheless, if we define τ_{100} and τ_N as simply the arithmetic average of the minimum and maximum value of the scattering time for their respective regions and τ_B as the value in the vicinity of the ⟨110⟩ axis then we obtain $\tau_N/\tau_B=1.8$ and $\tau_{100}/\tau_B=2.0$—very nearly in agreement with Dugdale and Firth's conclusion from Hall-effect data.

C. Origin of the anisotropy

The anisotropy may be understood by comparing the measured variation in scattering rate with the variations of the specific nature of the electron wave functions over the Cu Fermi surface. Figure 7 gives the relative amounts of s, p, and d components in the Cu electron wave func-

tion over the Fermi surface in the ⟨110⟩ plane. These fractions were obtained from augmented-plane-wave calculations.[22,23] One can compare the scattering anisotropy of Fig. 5 with the variation in wave function given in Fig. 7. As is clearly evident, there is a high correlation between the *d*-state fraction and the scattering-rate anisotropy. One can therefore conclude that the scattering potential introduced by the nickel scatters primarily the states with *d*-like symmetry. By comparison, the anisotropy seen in Cu(Al) correlates well with the variation in *p* state. As we noted elsewhere[6] the latter implies that the scattering potential introduced by the aluminum connects primarily *p* states with *p* states. An exactly analogous argument can be made to show that Ni results in scattering from *d* states to other *d* states.

In conclusion, we have used magnetic induced surface states to study the change in scattering rate upon alloying of Cu with Ni. We have found the results to be in good agreement with those obtained from dHvA measurements. Using these results we see that a two- or even three-band model is not entirely adequate to describe the Hall coefficient (or other transport properties) in alloys of Cu with Ni or Al. Instead, the continuously varying anisotropy around the Fermi surface must be accounted for. Finally, we see that in Cu there is a close correlation between the nature of the electron scattered by Ni and Al and the atomic nature of those two impurities.

ACKNOWLEDGMENTS

We wish to express our gratitude to the staff of the Metal Physics Branch, Naval Research Laboratory, Washington, D.C. for their assistance in this work. In particular, we are indebted to Dr. D. A. Papaconstantopoulos and his associates for providing wave-function data and insights. We also wish to acknowledge the valuable assistance and advice provided by Dr. R. Meussner regarding the metallurgical aspects of the program and Dr. G. N. Kamm regarding dHvA techniques.

[1]M. Springford, Adv. Phys. 20, 493 (1971).
[2]R. E. Prange and T. W. Nee, Phys. Rev. 168, 779 (1968).
[3]T. W. Nee, J. F. Koch, and R. E. Prange, Phys. Rev. 174, 758 (1968).
[4]J. F. Koch, in *Electrons in Metals,* Vol. I of *Solid State Physics* (The Simon Fraser University Lectures), edited by J. E. Cochran and R. E. Haering (Gordon and Breach, New York, 1968).
[5]M. S. Khaikan, Adv. Phys. 18, 493 (1971).
[6]A. J. Baratta and A. C. Ehrlich, Phys. Rev. B 24, 517 (1981).
[7]R. G. Poulsen, D. L. Randles, and M. Springford, J. Phys. F 4, 981 (1974).
[8]P. T. Coleridge, J. Phys. F 2, 1016 (1972).
[9]R. E. Doezema and J. F. Koch, Phys. Rev. B 6, 2071 (1972).
[10]R. E. Doezema and J. F. Koch, Phys. Rev. B 5, 3866 (1972).
[11]D. H. Lowndes, K. M. Miller, and M. Springford, Phys. Rev. Lett. 25, 1111 (1970).
[12]M. Springford, in *Electrons at the Fermi Surface,* edited by M. Springford (Cambridge University Press, New York, 1980), p. 362.
[13]G. N. Kamm, J. Appl. Phys. 49, 5951 (1978).
[14]R. E. Doezema and J. F. Koch, Phys. Condens. Matter, 19, 17 (1975).
[15]J. F. Koch and J. D. Jensen, Phys. Rev. 184, 643 (1969).
[16]W. J. Tegart, *The Electrolytic and Chemical Polishing of Metals in Research and Industry* (Pergamon, London, 1959).
[17]W. Jost, *Diffusion* (Academic, New York, 1960).
[18]P. T. Coleridge and I. M. Templeton, Can. J. Phys. 49, 2449 (1971).
[19]M. Tsuji, J. Phys. Soc. Jpn. 13, 979 (1958).
[20]J. S. Dugdale and L. D. Firth, J. Phys. C 2, 1272 (1969).
[21]J. S. Dugdale and Z. S. Basinski, Phys. Rev 157, 552 (1967); see also J. Bass, Adv. Phys. 21, 431 (1972).
[22]D. A. Papconstantopoulos, L. L. Boyer, B. M. Klein, A. R. Williams, V. L. Moruzzi, and J. F. Janak. Phys. Rev. B 15, 4221 (1977).
[23]D. A. Papaconstantopoulos (private communication).